

Distributed Time-Varying Graph Filtering

Elvin Isufi*, *Student Member, IEEE*, Andreas Loukas*, *Member, ACM*, Andrea Simonetto, *Member, IEEE*,
and Geert Leus, *Fellow, IEEE*

Abstract—One of the cornerstones of the field of signal processing on graphs are graph filters, direct analogues of classical filters, but intended for signals defined on graphs. This work brings forth new insights on the distributed graph filtering problem. We design a family of autoregressive moving average (ARMA) recursions, which (i) are able to *approximate* any desired graph frequency response, and (ii) give *exact* solutions for tasks such as graph signal denoising and interpolation.

The design philosophy, which allows us to design the ARMA coefficients independently from the underlying graph, renders the ARMA graph filters suitable in static and, particularly, time-varying settings. The latter occur when the graph signal and/or graph are changing over time. We show that in case of a time-varying graph signal our approach extends naturally to a two-dimensional filter, operating concurrently in the graph and regular time domains. We also derive sufficient conditions for filter stability when the graph and signal are time-varying. The analytical and numerical results presented in this paper illustrate that ARMA graph filters are practically appealing for static and time-varying settings, accompanied by strong theoretical guarantees.

Keywords— distributed graph filtering, signal processing on graphs, time-varying graph signals, time-varying graphs

I. INTRODUCTION

Due to their ability to capture the complex relationships present in many high-dimensional datasets, graphs have emerged as a favorite tool for data analysis. Indeed, in recent years we have seen significant efforts to extend classical signal processing methods to the graph setting, where, instead of a regular low-dimensional signal (e.g., a temporal or spatial signal), one is interested in graph signals, i.e., signals defined over the nodes of a graph [2]. The introduction of a Fourier-like transform for graph signals brought the tool to analyze these signals not only in the node domain, but also in the graph frequency domain [2]–[4]. The workhorses of graph signal analysis are *graph filters*. In a direct analogy to classical filters, graph filters process a graph signal by selectively amplifying its graph Fourier coefficients. This renders them ideal for a wide range of tasks, ranging from graph signal smoothing and denoising [5], [6], classification [7]–[9] and interpolation [10], segmentation [11], wavelet construction [12], and dictionary learning [13]—among others.

Distributed implementations of filters on graphs emerged as a way of increasing the scalability of computation [6],

[14]–[16]. Nevertheless, being inspired by finite impulse response (FIR) graph filters, these methods are sensitive to time variations, such as time-varying signals and/or graphs. An alternative approach, namely distributed infinite impulse response (IIR) graph filtering, was recently proposed [17], [18]. Compared to FIR graph filters, IIR filters allow the computation of a larger family of responses, and give exact rather than approximate solutions to the denoising [5] and interpolation [10] problems. Yet the issue of time variations has so far been unresolved.

In a different context, we introduced IIR filter design (in fact, prior to [18]) using an autoregressive process called the potential kernel [11], [19]. These graph filters were shown to facilitate information processing tasks in sensor networks, such as smoothing and event region detection, but, due to their ad-hoc design, they only accomplished a limited subset of filtering objectives. In this paper, we build upon our prior work to develop more general autoregressive moving average (ARMA) graph filters of any order, using parallel or periodic concatenations of the potential kernel. The design philosophy of these graph filters allows us to approximate any desired graph frequency response without knowing the structure of the underlying graph. In this way, we design the filter coefficients independently on the particular graph. This allows the ARMA filters to be *universally* applicable for any graph structure, and in particular when the graph varies over time, or when the graph structure is unknown to the designer.

Though ARMA graph filters belong to the class of IIR graph filters, they have a distinct design philosophy which bestows them the ability to filter graph signals not only in the graph frequency domain, but also in the regular temporal frequency domain (in case the graph signal is time-varying). Specifically, our design extends naturally to time-varying signals and graphs leading to two-dimensional ARMA filters: a filter in the graph domain as well as a filter in the time domain.

Our contributions are twofold:

(i) *Distributed graph filters (Sections III and IV)*. We propose two types of autoregressive moving average (ARMA) recursions, namely the parallel and periodic implementation, which attain a rational graph frequency response. Both methods are implemented distributedly, attain fast convergence, and have message and memory requirements that are linear in the number of graph edges and the approximation order. Using a variant of Shank’s method, we are able to design graph filters that approximate any desired graph frequency response. In addition, we give exact closed-form solutions for tasks such as graph signal denoising and interpolation.

(ii) *Time-varying graphs and signals (Section V)*. We begin

* Authors contributed equally in the preparation of this manuscript.

E. Isufi, A. Simonetto and G. Leus are with the faculty of Electrical Engineering, Mathematics and Computer Science, Delft University of Technology, 2826 CD Delft, The Netherlands. A. Loukas is with Department of Telecommunication Systems, TU Berlin, Germany. E-mails: {e.isufi-1, a.simonetto, g.j.t.leus}@tudelft.nl, a.loukas@tu-berlin.de. This manuscript presents a generalisation of [1]. This research was supported in part by STW under the D2S2 project from the ASSYS program (project 10561).

by providing a complete temporal characterization of ARMA graph filters w.r.t. time-varying graph signals. Our results show that the proposed recursions naturally extend to two-dimensional filters operating simultaneously in the graph-frequency domain and in the time-frequency domain. We also discuss the ARMA recursion behavior when both the graph and signal are time varying. Specifically, we provide sufficient conditions for filter stability, and show that a decomposition basis always exists (uniquely determined by the sequence of graph realizations), over which the filters achieve the same frequency response as in the static case.

Our results are validated by simulations in Section VI, and conclusions are drawn in Section VII.

Notation. We indicate a scalar valued variable by normal letters (i.e., a or A); a bold lowercase letter \mathbf{a} will indicate a vector variable and a bold upper case letter \mathbf{A} a matrix variable. We indicate by $|a|$ the absolute value of a and by $\|\mathbf{a}\|$ and $\|\mathbf{A}\|$ the 2-norm and the spectral norm of the vector \mathbf{a} and matrix \mathbf{A} , respectively. a_i is the i -th entry of \mathbf{a} , whereas A_{ij} is the (i, j) -th entry of \mathbf{A} . To characterize convergence, we adopt the term *linear convergence*, which asserts that a recursion converges to its stationary value exponentially with time (i.e., linearly in a logarithmic scale) [20]. We state the algorithmic message and memory complexity using the asymptotic $f(\cdot) = \Theta(g(\cdot))$ notation, which asserts that $f(\cdot)$ is bounded *both above and below* by $g(\cdot)$ asymptotically. This allows us to hide the architecture-dependent bit representation length of a floating point number and other (small) constants.

II. PRELIMINARIES

Consider a graph $G = (V, E)$ of N nodes and M edges, where V indicates the set of nodes and E the set of edges. Let \mathbf{x} be the graph signal defined on the graph nodes, whose i -th component $x_i \in \mathbb{R}$ represents the value of the signal at the i -th node, denoted as $u_i \in V$.

Graph Fourier Transform (GFT). The GFT transforms a graph signal \mathbf{x} into the graph frequency domain $\hat{\mathbf{x}}$: the forward and inverse GFTs of \mathbf{x} and $\hat{\mathbf{x}}$ are $\hat{x}_n = \langle \mathbf{x}, \phi_n \rangle$ and $x_n = \langle \hat{\mathbf{x}}, \phi_n \rangle$, where $\langle \cdot \rangle$ denotes the inner product. The vectors $\{\phi_n\}_{n=1}^N$ form an orthonormal basis and are commonly chosen as the eigenvectors of a graph Laplacian \mathbf{L} , such as the discrete Laplacian \mathbf{L}_d or Chung's normalized Laplacian \mathbf{L}_n . The corresponding eigenvalues are denoted as $\{\lambda_n\}_{n=1}^N$. For an extensive review of the properties of the GFT, we refer to [2], [3]. To avoid any restrictions on the generality of our approach, in the following we present our results for a *general basis matrix* \mathbf{L} . We only require that \mathbf{L} is *symmetric* and *local*: for all $i \neq j$, $L_{ij} = 0$ whenever u_i and u_j are not neighbors and $L_{ij} = L_{ji}$ otherwise.

Distributed graph filters. A *graph filter* \mathbf{F} is a linear operator that acts upon a graph signal \mathbf{x} by amplifying or attenuating its graph Fourier coefficients as

$$\mathbf{F}\mathbf{x} = \sum_{n=1}^N h(\lambda_n) \langle \mathbf{x}, \phi_n \rangle \phi_n. \quad (1)$$

Let λ_{\min} and λ_{\max} be the minimum and maximum eigenvalues of \mathbf{L} over *all* possible graphs. The graph frequency response

$h : [\lambda_{\min}, \lambda_{\max}] \rightarrow \mathbb{R}$ controls how much \mathbf{F} amplifies the signal component of each graph frequency

$$h(\lambda_n) = \langle \mathbf{F}\mathbf{x}, \phi_n \rangle / \langle \mathbf{x}, \phi_n \rangle. \quad (2)$$

We are interested in how we can filter a signal with a graph filter \mathbf{F} in a *distributed* way, having a user-provided frequency response $h^*(\lambda)$. Note that this prescribed $h^*(\lambda)$ is a continuous function in the graph frequency λ and describes the desired response for *any* graph. This approach brings benefits in those cases when the underlying graph structure is not known to the designer, or in cases the graph changes in time. The corresponding filter coefficients are thus independent of the graph and *universally* applicable. It is well known that we can *approximate* such an universal graph filter \mathbf{F} in a distributed way by using a K -th order polynomial of \mathbf{L} , for instance using Chebychev polynomials [6]. Define FIR_K as the K -th order approximation given by

$$\mathbf{F}_K = h_0 \mathbf{I} + \sum_{k=1}^K h_k \mathbf{L}^k, \quad (3)$$

where the coefficients h_i are found by minimizing the least-squares objective

$$\int_{\lambda} \left| \sum_{k=0}^K h_k \lambda^k - h^*(\lambda) \right|^2 d\lambda. \quad (4)$$

Observe that, in contrast to traditional graph filters, the order of the considered *universal* graph filters is not necessarily limited to N . By increasing K , we can approximate any filter with square integrable frequency response arbitrarily well. On the other hand, a larger FIR order implies a longer convergence time since each node requires information from all its K -hop neighbors to attain the desired filter response.

The computation of FIR_K is easily performed distributedly. Since $\mathbf{L}^K \mathbf{x} = \mathbf{L}(\mathbf{L}^{K-1} \mathbf{x})$, each node u_i can compute the K -th term from the values of the $(K-1)$ -th term in its neighborhood. The algorithm terminates after K iterations, and if a more efficient recursive implementation is used [6], in total, each node u_i exchanges $K \deg u_i$ values with its neighbors, meaning that, overall, the network exchanges $\Theta(MK)$ bits and at any time it needs to store $\Theta(M)$ bits (each node keeps track of the values of its neighbors at every iteration). However, FIR_K filters exhibit poor performance when the signal or/and graph are time-varying and when there exists asynchrony among the nodes. This is for two reasons: i) First, the distributed averaging is paused after K iterations, and thus the filter output is *not a steady state*. ii) Second, the input signal is only considered during the first iteration¹. To track time-varying signals, a new computation should be started at each time step. By running K filters in parallel however one increases the communication and memory complexities to $\Theta(K^2M)$ and $\Theta(KM)$ bits, respectively. In order to overcome these issues and provide a more solid foundation for graph signal processing, we study ARMA graph filters.

¹Throughout this paper we will assume that each iteration corresponds to one time instant.

III. ARMA GRAPH FILTERS

This section contains our main algorithmic contributions: First, Sections III-A and III-B present distributed algorithms for implementing filters with a complex rational graph frequency response

$$h(\lambda) = \frac{p_n(\lambda)}{p_d(\lambda)} = \frac{\sum_{k=0}^K b_k \lambda^k}{1 + \sum_{k=1}^K a_k \lambda^k}, \quad (5)$$

where $p_n(\lambda)$ and $p_d(\lambda)$ are the complex numerator and denominator polynomials of order K . Though both polynomials are presented here to be of the same order, this is not a limitation: different orders for $p_n(\lambda)$ and $p_d(\lambda)$ are achieved trivially by setting specific constants a_k or b_k to zero. For all our constructions, we characterize the convergence rate.

Before we proceed, a note is in order. The graph filtering problem has so far been defined in terms of a response $h(\lambda)$ having as domain the eigenvalues λ of the Laplacian \mathbf{L} . However, we find it useful to design our graph filters w.r.t. a translated version of \mathbf{L} defined as

$$\mathbf{M} = \varrho \mathbf{I} - \mathbf{L}, \quad \text{with } \varrho = \frac{\lambda_{\max} + \lambda_{\min}}{2}. \quad (6)$$

While using \mathbf{M} does not affect the filtering itself, it allows us to increase the stability region of the filters:

Filtering equivalence. According to Sylvester's matrix theorem, matrix \mathbf{M} has the same eigenvectors as \mathbf{L} , and the n -th eigenvalue μ_n of \mathbf{M} is a translation of the eigenvalue λ_n of \mathbf{L} , i.e., $\mu_n = \varrho - \lambda_n$. We can therefore attain the desired response $h(\lambda)$ by mapping it to the domain of \mathbf{M} 's eigenvalues: $g(\mu) = h(\varrho - \lambda)$. For instance, for the normalized Laplacian $g(\mu) = h(1 - \lambda)$, whereas for the standard Laplacian $g(\mu) = h(\lambda_{\max}/2 - \lambda)$.

Stability. By construction, $0 \leq \mu_{\max} = -\mu_{\min} \leq \varrho \leq \max\{|\lambda_{\max}|, |\lambda_{\min}|\}$, meaning that the spectral radius of \mathbf{M} is always smaller than or equal to the spectral radius of \mathbf{L} . In particular, for all positive semi-definite Laplacian matrices, $0 = \lambda_{\min} \leq \lambda_{\max}$ and the spectral radius decreases by a factor of two (since $\varrho = \lambda_{\max}/2$), leading to a significant increase of the stability region. This consideration plays a central role in the convergence of the ARMA filters, which will become more clear later on.

A. ARMA₁ graph filters

Before describing the full fledged ARMA_K filters, it helps to consider a 1-st order graph filter first. Besides being simpler in its construction, an ARMA₁ lends itself as the basic building block for creating filters with a rational frequency response of any order (cf. Section III-B). We obtain ARMA₁ filters as an extension of the potential kernel [19]. Consider the following 1-st order recursion

$$\mathbf{y}_{t+1} = \psi \mathbf{M} \mathbf{y}_t + \varphi \mathbf{x} \quad (7a)$$

$$\mathbf{z}_{t+1} = \mathbf{y}_{t+1} + c \mathbf{x}, \quad (7b)$$

for arbitrary \mathbf{y}_0 and where the coefficients ψ , φ and c are complex numbers (to be specified later on). For this recursion, we can prove our first result.

Theorem 1. The frequency response of the ARMA₁ is

$$g(\mu) = c + \frac{r}{\mu - p}, \quad \text{s.t. } |p| > \varrho \quad (8)$$

with residue r and pole p given by $r = -\varphi/\psi$ and $p = 1/\psi$, respectively. Recursion (7) converges to it linearly, irrespective of the initial condition \mathbf{y}_0 and graph Laplacian \mathbf{L} .

Proof. We can write the recursion (7a) at time t in the expanded form as

$$\mathbf{y}_t = (\psi \mathbf{M})^t \mathbf{y}_0 + \varphi \sum_{\tau=0}^{t-1} (\psi \mathbf{M})^\tau \mathbf{x}. \quad (9)$$

When $|\psi \varrho| < 1$ and as $t \rightarrow \infty$ this recursion approaches the steady state

$$\mathbf{y} = \lim_{t \rightarrow \infty} \mathbf{y}_t = \varphi \sum_{\tau=0}^{\infty} (\psi \mathbf{M})^\tau \mathbf{x} = \varphi (\mathbf{I} - \psi \mathbf{M})^{-1} \mathbf{x}, \quad (10)$$

irrespective of \mathbf{y}_0 . Based again on Sylvester's matrix theorem, the matrix $\mathbf{I} - \psi \mathbf{M}$ has the same eigenvectors as \mathbf{M} and its eigenvalues are equal to $1 - \psi \mu_n$. It is also well known that invertible matrices have the same eigenvectors as their inverse and eigenvalues that are the inverse of the eigenvalues of their inverse. Thus,

$$\mathbf{z} = \lim_{t \rightarrow \infty} \mathbf{z}_t = \mathbf{y} + c \mathbf{x} = \sum_{n=1}^N \left(c + \frac{\varphi}{1 - \psi \mu_n} \right) \hat{x}_n \phi_n, \quad (11)$$

and the desired frequency response (8) follows by simple algebra. We arrive at (11) by considering a specific realization of \mathbf{M} , thus the set of eigenvalues $\mu_n \in [\mu_{\min}, \mu_{\max}]$ is discrete. However, the same result is achieved for every other graph realization matrix \mathbf{M} with potentially a different set of eigenvalues, still in $[\mu_{\min}, \mu_{\max}]$. Thus, we can write (8) for all $\mu \in [\mu_{\min}, \mu_{\max}]$. \square

Recursion (7) leads to a very efficient distributed implementation of a graph filter with 1-st order rational frequency response: at each iteration t , each node u_i updates its value $y_{t,i}$ based on its local signal x_i and a weighted combination of the values $y_{t-1,j}$ of its neighbors u_j . Since each node must exchange its value with each of its neighbors, the message/memory complexity at each iteration is $\Theta(M)$ bits.

B. ARMA_K graph filters

Next, we use ARMA₁ as a building block to derive distributed graph filters with a more complex frequency response. We present two constructions: The first uses a *parallel* bank of K ARMA₁ filters, attaining linear convergence at the price of exchanging and storing $\Theta(KM)$ bits per iteration. The second uses *periodic* coefficients in order to reduce the number of bits exchanged to $\Theta(M)$, while maintaining similar convergence properties.

Parallel ARMA_K filters. A larger variety of filter responses can be obtained by adding the outputs of a parallel ARMA₁ filter bank. Let's denote with the superscript (k) the terms that correspond to the k -th ARMA₁ filter for $k = 1, 2, \dots, K$.

With this notation in place, the output z_t of the ARMA $_K$ filter at time instant t is

$$\mathbf{y}_{t+1}^{(k)} = \psi^{(k)} \mathbf{M} \mathbf{y}_t^{(k)} + \varphi^{(k)} \mathbf{x} \quad (12a)$$

$$\mathbf{z}_{t+1} = \sum_{k=1}^K \mathbf{y}_{t+1}^{(k)} + c \mathbf{x}, \quad (12b)$$

where $\mathbf{y}_0^{(k)}$ is arbitrary.

Theorem 2. The frequency response of a parallel ARMA $_K$ is

$$g(\mu) = c + \sum_{k=1}^K \frac{r_k}{\mu - p_k} \quad \text{s.t. } |p_k| > \varrho, \quad (13)$$

with the residues $r_k = -\varphi^{(k)}/\psi^{(k)}$ and poles $p_k = 1/\psi^{(k)}$. Recursion (12) converges to it linearly, irrespective of the initial condition $\mathbf{y}_0^{(k)}$ and graph Laplacian \mathbf{L} .

Proof. Follows straightforwardly from Theorem 1. \square

The frequency response of a parallel ARMA $_K$ is therefore a rational function with numerator and denominator polynomials of order K (presented here in a partial fraction form). In addition, since we are simply running K ARMA $_1$ filters in parallel, the communication and memory complexities are K times that of the ARMA $_1$ graph filter.

Periodic ARMA $_K$ filters. We can decrease the memory requirements of the parallel implementation by letting the filter coefficients periodically vary in time. Our periodic filters take the following form

$$\mathbf{y}_{t+1} = (\theta_t \mathbf{I} + \psi_t \mathbf{M}) \mathbf{y}_t + \varphi_t \mathbf{x} \quad (14a)$$

$$\mathbf{z}_{t+1} = \mathbf{y}_{t+1} + c \mathbf{x}, \quad (14b)$$

where \mathbf{y}_0 is arbitrary, the output \mathbf{z}_{t+1} is valid every K iterations, and coefficients $\theta_t, \psi_t, \varphi_t$ are periodic with period K : $\theta_t = \theta_{t-iK}, \psi_t = \psi_{t-iK}, \varphi_t = \varphi_{t-iK}$, with i an integer in $[0, t/K]$.

Theorem 3. The frequency response of a periodic ARMA $_K$ filter is

$$g(\mu) = c + \frac{\sum_{k=0}^{K-1} \left(\prod_{\tau=k+1}^{K-1} \theta_\tau + \psi_\tau \mu \right) \varphi_k}{1 - \left(\prod_{k=0}^{K-1} \theta_k + \psi_k \mu \right)}, \quad (15)$$

s.t. the stability constraint $|\prod_{\tau=0}^{K-1} \theta_\tau + \psi_\tau \varrho| < 1$. Recursion (14) converges to it linearly, irrespective of the initial condition \mathbf{y}_0 and graph Laplacian \mathbf{L} .

Proof. Define matrices $\mathbf{\Gamma}_t = \theta_t \mathbf{I} + \psi_t \mathbf{M}$ and $\mathbf{\Phi}_{(t_1, t_2)} = \mathbf{\Gamma}_{t_1} \mathbf{\Gamma}_{t_1-1} \cdots \mathbf{\Gamma}_{t_2}$ if $t_1 \geq t_2$, whereas $\mathbf{\Phi}_{(t_1, t_2)} = \mathbf{I}$ otherwise. The output at the end of each period can be re-written as a time-invariant system

$$\mathbf{y}_{(i+1)K} = \overbrace{\mathbf{\Phi}_{(K-1, 0)}}^{\triangleq \mathbf{A}} \mathbf{y}_{iK} + \overbrace{\sum_{k=0}^{K-1} \mathbf{\Phi}_{(K-1, k+1)} \varphi_k \mathbf{x}}^{\triangleq \mathbf{B}} \quad (16a)$$

$$\mathbf{z}_{(i+1)K} = \mathbf{y}_{(i+1)K} + c \mathbf{x}. \quad (16b)$$

Both \mathbf{A} and \mathbf{B} have the same eigenvectors ϕ_n as \mathbf{M} (and \mathbf{L}). As such, when for \mathbf{A} 's maximum eigenvalue holds that $|\lambda_{\max}(\mathbf{A})| < 1$, the steady state of (16b) is

$$\mathbf{z} = (\mathbf{I} - \mathbf{A})^{-1} \mathbf{B} \mathbf{x} + c \mathbf{x} = \sum_{n=1}^N \left(c + \frac{\lambda_n(\mathbf{B})}{1 - \lambda_n(\mathbf{A})} \right) \hat{x}_n \phi_n. \quad (17)$$

To derive the exact response, notice that

$$\lambda_n(\mathbf{\Phi}_{(t_1, t_2)}) = \prod_{\tau=t_1}^{t_2} \lambda_n(\mathbf{\Gamma}_\tau) = \prod_{\tau=t_1}^{t_2} (\theta_\tau + \psi_\tau \mu_n), \quad (18)$$

which, by the definition of \mathbf{A} and \mathbf{B} , yields the desired frequency response. The linear convergence rate and stability condition follow from the linear convergence of (16b) to \mathbf{y} with rate $|\lambda_{\max}(\mathbf{A})|$. \square

By some algebraic manipulation, we can see that the frequency response of periodic ARMA $_K$ filters is also a rational function of order K .

IV. ARMA FILTER DESIGN

In the rest of this section we focus on selecting the coefficients of our filters. We begin by showing how to approximate any given frequency response with an ARMA filter, using a variant of Shank's method [21]. This approach gives us stable filters, ensuring the same selectivity as the universal FIR graph filters. Section IV-B then provides explicit (and exact) filter constructions for two graph signal processing problems which were up-to-now only approximated: *graph signal denoising* and *interpolation* [6], [22] and [10].

A. The Filter Design Problem

Given a graph frequency response $g^* : [\mu_{\min}, \mu_{\max}] \rightarrow \mathbb{R}$ and filter order K , our objective is to find the complex polynomials $p_n(\mu)$ and $p_d(\mu)$ of order K that minimize

$$\int_{\mu} \left| \frac{p_n(\mu)}{p_d(\mu)} - g^*(\mu) \right|^2 d\mu = \int_{\mu} \left| \frac{\sum_{k=0}^K b_k \mu^k}{1 + \sum_{k=1}^K a_k \mu^k} - g^*(\mu) \right|^2 d\mu \quad (19)$$

while ensuring that the chosen coefficients result in a stable system (see constraints in Theorems 2 and 3). From $p_n(\mu)/p_d(\mu)$ one computes the filter coefficients $(\psi^{(k)}, \varphi^{(k)}, c$ or θ_t, ψ_t, c) by algebraic manipulation.

Remark 1. Whereas g^* is a function of μ , the desired frequency response $h^* : [\lambda_{\min}, \lambda_{\max}] \rightarrow \mathbb{R}$ is a function of λ . We attain $g^*(\mu)$ by simply mapping the user-provided response $h^*(\lambda)$ to the domain of μ : $g^*(\mu) = h^*(\varrho - \lambda)$, where $\varrho = (\lambda_{\max} + \lambda_{\min})/2$ is a constant determined a-priori.

Remark 2. Even if we constrain ourselves to pass-band filters and we consider only the set of \mathbf{L} for which $\varrho = 1$, it is impossible to design our coefficients based on classical design methods developed for IIR filters (e.g., Butterworth, Chebyshev). The same issue is present also using a rational fitting approach, e.g., Padé and Prony's method. This is because the

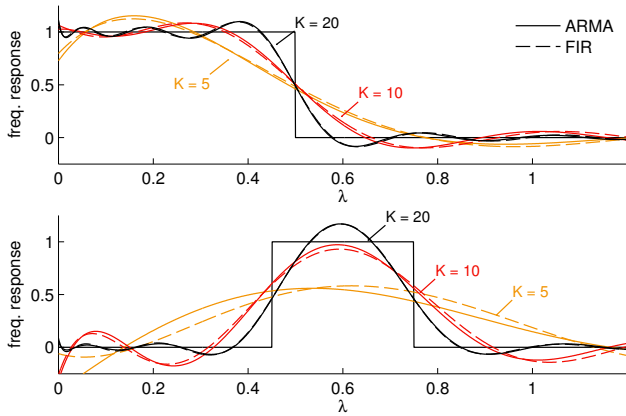


Fig. 1. The frequency response of ARMA_K filters designed by Shank's method and the FIR responses of corresponding order. Here, h^* is a step function (top) and a window function (bottom).

stability constraint of ARMA_K is different from classical filter design, where the poles of the transfer function must lie within (not outside) the unit circle.

To illustrate this remark, consider the Butterworth-like graph frequency response $h(\lambda) = (1 + (\lambda/\lambda_c)^K)^{-1}$, where λ_c is the desired cut-off frequency. For $K = 2$, one finds that the poles lie at $\pm\lambda_c$. Thus, the stability of these filters is dependent on the cut-off frequency which does not always guarantee stable filters.

Design method. Similar to Shank's method, we approximate the filter coefficients as follows:

Denominator. Determine a_k for $k = 1, \dots, K$ by finding a $\hat{K} > K$ order polynomial approximation $\hat{g}(\mu) = \sum_{k=0}^{\hat{K}} g_k \mu^k$ of $g^*(\mu)$ using polynomial regression, and solving the coefficient-wise system of equations $p_d(\mu)\hat{g}(\mu) = p_n(\mu)$.

Numerator. Determine b_k for $k = 1, \dots, K$ by solving the least-squares problem of minimizing $\int_{\mu} |p_n(\mu)/p_d(\mu) - g^*(\mu)|^2 d\mu$, w.r.t. $p_n(\mu)$.

The method is also suitable for numerator and denominator polynomials of different orders. We advocate however the use of equal orders, because it yields the highest approximation accuracy for a given communication/memory complexity.

The most crucial step is the approximation of the denominator coefficients. By fitting $p_d(\mu)$ to $\hat{g}(\mu)$ instead of $g(\mu)$, we are able to compute coefficients a_k independently of b_k . Increasing $\hat{K} \gg K$ often leads to a (slight) increase in accuracy, but at the price of slower convergence and higher sensitivity to numerical errors (such as those caused by packet loss). Especially for sharp functions, such as the ones shown in Fig. 1, a high order polynomial approximation results in very large coefficients, which affect the numerical stability of the filters and push the poles closer to the unit circle. For this reason, in the remainder of this paper we set $\hat{K} = K + 1$.

Though the proposed design method does not come with theoretical stability guarantees, it has been found to consistently produce stable filters. Fig. 1 illustrates in solid lines the frequency responses of three ARMA_K filters ($K = 5, 10, 20$), designed to approximate a step function (top) and a window

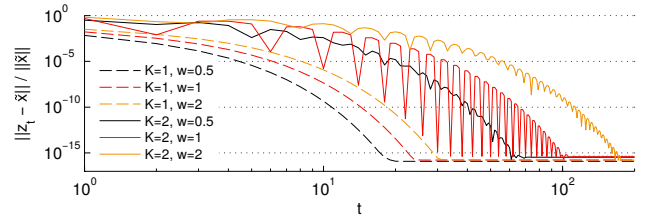


Fig. 2. Convergence of denoising parallel ARMA_K filter for $K = 1, 2$ and $w = 0.5, 1, 2$. The filtering error is $\|z_t - \tilde{x}\|/\|\tilde{x}\|$, where for each parameter pair (K, w) , \tilde{x} is the solution of the denoising problem, and z_t is the filter output after t rounds. The residual error is a consequence of the computer's bounded numerical precision.

function (bottom). ARMA responses closely approximate the optimal FIR responses for the corresponding orders (dashed lines). For completeness and reproducibility, we include in Table I the filter coefficients of a parallel ARMA_K filter approximating the step function with cut-off $\lambda_c = 0.5$ (i.e., filter response equal to 1 for $\lambda < \lambda_c$ and zero otherwise) for $K = 3, 5, 7$. Higher order filters are omitted due to space considerations.

B. Exact and Universal Graph Filter Constructions

We proceed to present exact (and in certain cases explicit) graph filter constructions for the graph denoising and interpolation problems. In contrast to previous work, the proposed filters are *universal*, that is they are designed without knowledge of the graph structure. Indeed, the filter coefficients are found independently from the eigenvalues of the graph Laplacian. This makes the ARMA filters suitable for any graph, and ideal for cases when the graph structure is unknown or when the $O(n^3)$ complexity of the eigenvalue decomposition becomes prohibitive.

Tikhonov-based denoising. Given a noisy signal $t = x + n$, where x is the true signal and n is noise, the objective is to recover x [2], [6], [22]. When x is smooth w.r.t. the graph, denoising can be formulated as the regularized problem

$$\tilde{x} = \underset{x \in \mathbb{R}^n}{\text{argmin}} \|x - t\|_2^2 + w x^\top L^K x, \quad (20)$$

where the first term asks for a denoised signal that is close to t , and the second uses the quadratic form of L^K to penalize signals that are not smooth. The positive regularization weight w allows us to trade-off between the two terms of the objective function. Being a convex problem, the global minimum \tilde{x} is found by setting the gradient to zero

$$\tilde{x} = (I + wL^K)^{-1} t = \sum_{n=1}^N \frac{1}{1 + w\lambda_n^K} \langle t, \phi_n \rangle \phi_n. \quad (21)$$

It follows that the denoised signal is the output of an ARMA_K with frequency response $h(\lambda) = (1 + w\lambda^K)^{-1}$, which, expressed in the domain of M 's spectrum, is

$$g(\mu) = \frac{1}{1 + w(\varrho - \mu)^K} = \frac{1}{\prod_{k=1}^K (\mu - p_k)} \quad (22)$$

with $p_k = \varrho - e^{i\gamma_k}/\sqrt[k]{w}$ for $\gamma_k = (2k + 1)\pi/K$. The denominator coefficients $\psi^{(k)}$ of the corresponding parallel ARMA_K filter for (22) can be found as $\psi^{(k)} = 1/p_k$. Meanwhile, the numerator coefficients $\varphi^{(k)}$ are found in two

TABLE I
RESIDUES r_k AND POLES p_k OF PARALLEL ARMA $_K$ FILTER, FOR $K = 3, 5$ AND 7 .

order	r_0, p_0	r_1, p_1	r_2, p_2	r_3, p_3	r_4, p_4	r_5, p_5	r_6, p_6
K=3	10.954 + 0 <i>i</i> , -6.666 + 0 <i>i</i>	1.275 + 1.005 <i>i</i> , 0.202 + 1.398 <i>i</i>	1.275 - 1.005 <i>i</i> , 0.202 - 1.398 <i>i</i>	-	-	-	-
K=5	-7.025 + 0 <i>i</i> , -3.674 + 0 <i>i</i>	-1.884 - 1.298 <i>i</i> , -0.420 + 1.269 <i>i</i>	-1.884 + 1.298 <i>i</i> , -0.420 - 1.269 <i>i</i>	1.433 - 1.568 <i>i</i> , 0.703 + 1.129 <i>i</i>	1.433 + 1.568 <i>i</i> , 0.703 + 1.129 <i>i</i>	-	-
K=7	-46.398 + 0 <i>i</i> , -3.842 + 0 <i>i</i>	-20.207 - 8.343 <i>i</i> , 0.102 + 1.427 <i>i</i>	-20.207 + 8.343 <i>i</i> , 0.102 + 1.427 <i>i</i>	-5.205 + 4.946 <i>i</i> , -0.785 + 1.128 <i>i</i>	-5.205 - 4.946 <i>i</i> , -0.785 + 1.128 <i>i</i>	3.124 - 10.622 <i>i</i> , 0.902 + 1.011 <i>i</i>	3.124 + 10.622 <i>i</i> , 0.902 - 1.011 <i>i</i>

steps: (i) express (22) in the partial form as in (13) to find the residuals r_k and (ii) take $\varphi^{(k)} = -r_k \psi^{(k)}$. By solving the stability condition inequality $|\psi^{(k)}| = |1/p_k| \leq 1/|\mu_{max}|$, we find that the denoising parallel ARMA $_K$ is stable as long as

$$(\varrho^2 - \mu_{max}^2) \sqrt[K]{w^2} - 2\varrho \cos \gamma_k \sqrt[K]{w} + 1 \geq 0. \quad (23)$$

For the normalized and random-walk normalized Laplacian matrices, $\varrho^2 = \mu_{max}^2 = 1$, and the stability condition simplifies to

$$2 \cos \gamma_k \sqrt[K]{w} \leq 1, \quad (24)$$

which is always met for the standard choices of $K = 1$ (quadratic regularization) and $K = 2$ (total variation). For these values of K , and for different values of the regularized weight w , we show in Fig. 2 the normalized error between the output of the ARMA $_K$ recursion and the solution of the optimization problem (20), as a function of time.

Wiener-based denoising. When the statistical properties of the graph signal and noise are available, it is common to opt for a Wiener filter, i.e., the linear filter that minimizes the mean-squared error (MSE)

$$\tilde{\mathbf{F}} = \min_{\mathbf{F} \in \mathbb{R}^{n \times n}} \mathbb{E} \left[\|\mathbf{F}\mathbf{t} - \mathbf{x}\|_2^2 \right] \text{ and } \tilde{\mathbf{x}} = \tilde{\mathbf{F}}\mathbf{t} \quad (25)$$

where as before $\mathbf{t} = \mathbf{x} + \mathbf{n}$ is the graph signal which has been corrupted with additive noise. It is well known that, when \mathbf{x} and \mathbf{n} are zero-mean with covariance $\Sigma_{\mathbf{x}}$ and $\Sigma_{\mathbf{n}}$, respectively, the solution of (25) is

$$\tilde{\mathbf{x}} = \Sigma_{\mathbf{x}} (\Sigma_{\mathbf{x}} + \Sigma_{\mathbf{n}})^{-1} \mathbf{t}. \quad (26)$$

The above linear system can be solved by a graph filter when matrices $\Sigma_{\mathbf{x}}$ and $\Sigma_{\mathbf{n}}$ share the eigenvectors of the Laplacian matrix \mathbf{L} . Denote by $\sigma_{\mathbf{x}}(\lambda_n) = \phi_n^T \Sigma_{\mathbf{x}} \phi_n$ the eigenvalue of matrix $\Sigma_{\mathbf{x}}$ which corresponds to the n -th eigenvector of \mathbf{L} , and correspondingly $\sigma_{\mathbf{n}}(\lambda_n) = \phi_n^T \Sigma_{\mathbf{n}} \phi_n$. We then have that

$$\tilde{\mathbf{x}} = \sum_{n=1}^n \frac{\sigma_{\mathbf{x}}(\lambda_n)}{\sigma_{\mathbf{x}}(\lambda_n) + \sigma_{\mathbf{n}}(\lambda_n)} \langle \mathbf{t}, \phi_n \rangle \phi_n. \quad (27)$$

It follows that, when $\sigma_{\mathbf{x}}(\lambda)$ and $\sigma_{\mathbf{n}}(\lambda)$ are rational functions (of λ) of order K , the Wiener filter corresponds to an ARMA $_K$ graph filter. Notice that the corresponding filters are still universal, as the ARMA $_K$ coefficients depend on the rational functions $\sigma_{\mathbf{x}}(\lambda)$ and $\sigma_{\mathbf{n}}(\lambda)$, but not on the specific eigenvalues of the graph Laplacian.

Let us illustrate the above with an example. Suppose that \mathbf{x} is normally distributed with covariance equal to the pseudoinverse of the Laplacian \mathbf{L}^+ . This is a popular and well understood model for smooth signals on graphs with strong connections to Gaussian Markov random fields [23]. In addition, let the noise be white with variance w . Substituting this into (27), we find

$$\tilde{\mathbf{x}} = \sum_{n=1}^n \frac{1}{1 + w\lambda_n} \langle \mathbf{t}, \phi_n \rangle \phi_n, \quad (28)$$

which is identical to the Tikhonov-based denoising for $K = 1$ and corresponds to an ARMA $_1$ with $\psi = \phi = 1/(1 + \varrho w)$.

Graph signal interpolation. Suppose that only r out of the N values of a signal \mathbf{x} are known, and let \mathbf{t} be the $N \times 1$ vector which contains the known values and zeros otherwise. Under the assumption of \mathbf{x} being smooth w.r.t. \mathbf{L} , we can estimate the unknowns by the regularized problem

$$\tilde{\mathbf{x}} = \operatorname{argmin}_{\mathbf{x} \in \mathbb{R}^n} \|\mathbf{S}(\mathbf{x} - \mathbf{t})\|_2^2 + w \mathbf{x}^T \mathbf{L}^K \mathbf{x}, \quad (29)$$

where \mathbf{S} is the diagonal matrix with $S_{ii} = 1$ if x_i is known and $S_{ii} = 0$ otherwise. Such formulations have been used widely, both in the context of graph signal processing [10], [24] and earlier by the semi-supervised learning community [9], [25]. Similar to (20), this optimization problem is convex and its global minimum is found as

$$\tilde{\mathbf{x}} = (\mathbf{S} + w\mathbf{L}^K)^{-1} \mathbf{t}. \quad (30)$$

Most commonly, $K = 1$, and $\tilde{\mathbf{x}}$ can be re-written as

$$\tilde{\mathbf{x}} = \left((1 + \hat{\varrho})\mathbf{I} - \hat{\mathbf{M}} \right)^{-1} \mathbf{t} = \sum_{n=1}^N \frac{1}{1 + \hat{\varrho} - \hat{\mu}_n} \langle \mathbf{t}, \hat{\phi}_n \rangle \hat{\phi}_n. \quad (31)$$

which is an ARMA $_1$ filter designed for the modified Laplacian matrix $\hat{\mathbf{L}} = \mathbf{S} - \mathbf{I} + w\mathbf{L}$ and thus $\hat{\varrho} = (\hat{\lambda}_{max} + \hat{\lambda}_{min})/2$, with $\hat{\lambda}_{max}$ and $\hat{\lambda}_{min}$ the maximum and minimum eigenvalues of $\hat{\mathbf{L}}$ over all possible graphs. Further, $\hat{\mathbf{M}} = \hat{\varrho}\mathbf{I} - \hat{\mathbf{L}}$ and $(\hat{\mu}_n, \hat{\phi}_n)$ is the n -th eigenpair of $\hat{\mathbf{M}}$. For larger values of K , the interpolation cannot be computed distributedly using ARMA filters. That is because the corresponding basis matrix $\hat{\mathbf{L}} = \mathbf{S} + w\mathbf{L}^K$ cannot be appropriately factorized into a series of local matrices.

V. TIME-VARIATIONS

We have at this point characterized the filtering and convergence properties of ARMA graph filters for static inputs. But do these properties hold when the graph and signal are a function of time? In the following, we characterize ARMA graph filters with respect to time-variations in the graph signal (cf. Section V-A), as well as in the graph (cf. Section V-B).

A. Joint Graph and Temporal Filters

To understand the impact of graph signal dynamics we broaden the analysis to a two-dimensional domain: the first dimension, as before, captures the graph (based on the graph Fourier transform), whereas the second dimension captures time (based on the Z-transform). This technique allows us to provide a complete characterization of the ARMA filter subject to time-variations. First, we show that the ARMA filter output remains close to the correct time-varying solution (under sufficient conditions on the input), which implies that our algorithms exhibit a certain robustness to dynamics. Further, we realize that ARMA graph filters operate along both the graph and temporal dimensions. We find that a graph naturally dampens temporal frequencies in a manner that depends on its spectrum. Exploiting this finding, we extend the ARMA designs presented in Section III so as to also allow a measure of control over the temporal frequency response of the filters.

As previously, we start our exposition with the ARMA₁ recursion (7), but now the input graph signal x_t is time dependent (thus, indexed with the subscript t)

$$\mathbf{y}_{t+1} = \psi \mathbf{M} \mathbf{y}_t + \varphi \mathbf{x}_t \quad (32a)$$

$$\mathbf{z}_{t+1} = \mathbf{y}_{t+1} + c \mathbf{x}_t. \quad (32b)$$

The dimension of the above recursion can be reduced by restricting the input graph signal to lie in the subspace of an eigenvector ϕ with associated eigenvalue μ , i.e., $\mathbf{x}_t = x_t \phi$, where now x_t is a scalar². By orthogonality of the basis, the filter only alters the magnitude x_t and not the direction of \mathbf{x}_t . Therefore, (32) is equivalent to

$$y_{t+1} = \psi \mu y_t + \varphi x_t \quad (33a)$$

$$z_{t+1} = y_{t+1} + c x_t, \quad (33b)$$

where $x_t, y_t, z_t \in \mathbb{R}$ are simply the magnitudes of the vectors $\mathbf{x}_t, \mathbf{y}_t, \mathbf{z}_t \in \mathbb{C}^n$ lying on the eigenspace of ϕ , and we can write $\mathbf{y}_t = y_t \phi$ and $\mathbf{z}_t = z_t \phi$. Taking the Z-transform on both sides, we obtain the joint graph and temporal frequency transfer function

$$H(z, \mu) = \frac{\varphi z^{-1}}{1 - \psi \mu z^{-1}} + c z^{-1}. \quad (34)$$

It can be shown that the joint impulse response of the filter is

$$\mathbf{h}_{t+1}(\mu) = (\varphi(\psi \mu)^t + c) \phi, \quad (35)$$

from which we deduce that the region of convergence (ROC) of the filter is $\{|z| > |\psi \mu|\}$, for all μ and that the filter is causal.

²This is a standard way to derive the frequency response of a system.

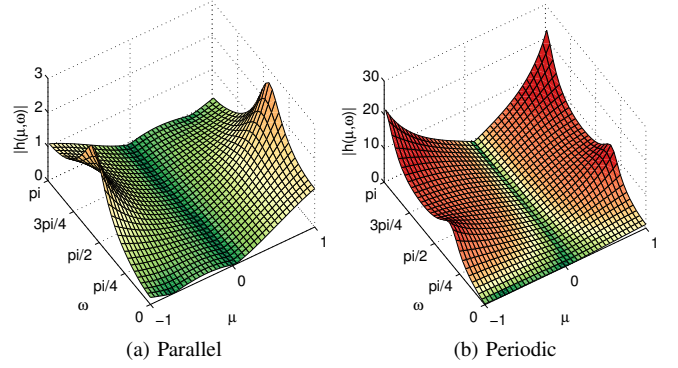


Fig. 3. The joint graph and temporal frequency response of a parallel and a periodic graph filter, both designed to approximate an ideal low pass (step) response with (translated) cut-off frequency $\mu_c = 0.5$ and $K = 3$.

The joint transfer function characterizes completely the behavior of ARMA₁ graph filters for an arbitrary yet time-invariant graph: when $z \rightarrow 1$, we return to the constant \mathbf{x} result and stability condition of Theorem 1, while for all other z we obtain the standard frequency response as well as the graph frequency one. As one can see, recursion (32) is an ARMA₁ filter in the graph domain as well as in the time domain. Observe also that the poles of $H(z, \mu)$ obey the fixed relationship $z = \mu \psi$. This yields an interesting insight: the temporal frequency response of the filter differs along each graph frequency μ , meaning that temporal dynamics affecting signals lying in low graph frequency eigenspaces are dampened to a smaller extent.

As Theorems 4 and 5 below show, the results are readily generalized to higher order filters.

Theorem 4. The joint graph and temporal frequency transfer function of a parallel ARMA_K is

$$H(z, \mu) = \sum_{k=1}^K \frac{\varphi^{(k)} z^{-1}}{1 - \psi^{(k)} \mu z^{-1}} + c z^{-1}, \quad (36)$$

subject to the stability conditions of Theorem 2.

Theorem 5. The joint graph and temporal frequency transfer function of a periodic ARMA_K is

$$H(z, \mu) = \frac{\sum_{k=0}^{K-1} \left(\prod_{\tau=k+1}^{K-1} \theta_\tau + \psi_\tau \mu \right) \varphi_k z^{k-K}}{1 - \left(\prod_{\tau=0}^{K-1} \theta_\tau + \psi_\tau \mu \right) z^{-K}} + c z^{-1}, \quad (37)$$

subject to the stability conditions of Theorem 3.

(The proofs are deferred to the appendix.)

As in the first order case, Theorems 4 and 5 describe completely the behavior of the parallel and periodic implementations. We can see that both filters are ARMA_K filters in the graph and temporal domain. In particular, the parallel and periodic filters have up to K distinct poles abiding respectively to

$$z = \psi^{(k)} \mu \quad \text{and} \quad z = \sqrt[K]{\prod_{\tau=0}^{K-1} \theta_\tau + \psi_\tau \mu}. \quad (38)$$

To provide further insight, Fig. 3 plots the joint graph and temporal frequency response of a parallel and a periodic graph filter of third order, both designed to approximate an ideal low pass response with cut-off frequency $\lambda_c = 0.5$. In contrast to the rest of the figures in this paper, this figure depicts the translated graph frequency $\mu = \rho - \lambda$ (with $\rho = 1$), meaning that higher values of μ correspond to smaller variation terms. The temporal axis on the other hand measures the temporal frequency ω such that, for $\omega = 0$, one obtains the standard graph frequency response. To increase visibility, the figure only shows frequencies in $[0, \pi]$ (between π and 2π the response is symmetric to what is shown here).

We make two observations: *First, both graph filters dampen less temporal variations of low graph frequency eigenspaces (similar to ARMA₁).* Whereas for graph signals lying in eigenspaces with $\mu \approx 0$ all temporal frequencies are damped, as the magnitude of μ increases, the magnitude of temporal fluctuations in the output becomes progressively larger. This is a phenomenon that transcends the filter implementation (parallel or periodic) and the particular coefficients chosen and is due to the multiplicative relation of the response poles. *Second, the parallel concatenation of ARMA₁ filters results in a more stable implementation that is more fit to tolerate temporal dynamics than in the periodic case.* As shown in Figure 3b, for $|\mu| = 1$, temporal fluctuations with frequencies exceeding $\pi/4$ cause the periodic filter output to blow up by an order of magnitude, effectively rendering the periodic implementation unusable. The poor stability of the periodic implementation is also seen from (37), where the θ_τ terms tend to push the poles closer to the unit circle, and it is the price to pay for its small memory requirements.

Due to its superior stability properties and convenient form (less coefficients and simpler design), we suggest the parallel implementation for dealing with time-varying graph signals.

B. Time-Varying Graphs and Signals

Time variations on the graph topology bring new challenges to the graph filtering problem. *First, they render approaches that rely on knowledge of the graph spectrum ineffective.* Approaches which ensure stability by designing the poles to lie outside the set of the Laplacian eigenvalues of a given graph, may lead to unstable filters in a time-varying graph context when the eigenvalues of the new graph realization match one of the poles. Due to their different design philosophy, the presented ARMA graph filters handle naturally the aforementioned issues. We can, for instance, think that the different graph realizations among time enjoy an upper bound on their maximum eigenvalue λ_{max} . In case this is not possible, or difficult to determine, we can always work with the normalized Laplacian and thus take $\lambda_{max} = 2$. In this way, by designing the filter coefficients in order to ensure stability w.r.t. λ_{max} , we automatically impose stability for all different graph realizations over time. Furthermore, by designing once the filter coefficients for a continuous range of frequencies, the ARMA recursions also preserve the desired frequency response for different graph realizations.

The second major challenge is characterizing the graph filter behavior. Time-varying affine systems are notoriously

difficult to analyze when they possess no special structure [26]. To this end, we devise a new methodology for time-varying graph filter analysis. We show that a decomposition basis always exists, over which ARMA₁ graph filters (and as a consequence parallel ARMA_K filters) have the same frequency response as in the static case. Furthermore, this basis depends only on the sequence of graph realizations.

In case of a time-varying graph topology as well as a time-varying graph signal the ARMA₁ recursion (7) can be written as

$$\mathbf{y}_{t+1} = \psi \mathbf{M}_t \mathbf{y}_t + \varphi \mathbf{x}_t \quad (39a)$$

$$\mathbf{z}_{t+1} = \mathbf{y}_{t+1} + \mathbf{c} \mathbf{x}_t, \quad (39b)$$

where the time-varying graph is shown by indexing \mathbf{M}_t with the subscript t . Expanding the recursion we find that, for any sequence of graph realizations $\{G_0, G_1, \dots, G_t\}$ with corresponding shifted Laplacians $\{\mathbf{M}_0, \mathbf{M}_1, \dots, \mathbf{M}_t\}$, the output signal is given by

$$\mathbf{z}_{t+1} = \psi^{t+1} \Phi(t, 0) \mathbf{y}_0 + \varphi \sum_{\tau=0}^t \psi^\tau \Phi(t, t-\tau+1) \mathbf{x}_{t-\tau} + \mathbf{c} \mathbf{x}_t, \quad (40)$$

where $\Phi(t, t') = \prod_{i=t'}^t \mathbf{M}_i$ for $t \geq t'$, and $\Phi(t, t') = \mathbf{I}$ otherwise.

Since the output \mathbf{z}_t depends on the entire sequence of graph realizations, the spectrum of any individual Laplacian is insufficient as to derive the graph frequency of the filter. To extend the spectral analysis to the time-varying setting we define a joint shifted Laplacian matrix \mathbf{M}_N that encompasses all the individual shifted graph Laplacians. The spectrum of \mathbf{M}_N will then serve as the basis for our time-varying graph Fourier transform. To proceed, define $\mathbf{P}(t)$ to be the $(t+1) \times (t+1)$ cyclic shift matrix and construct $\mathbf{M}_N(t)$ as the $N(t+1) \times N(t+1)$ permuted block-diagonal matrix

$$\mathbf{M}_N(t) = \text{blkdiag}(\mathbf{M}_0, \mathbf{M}_1, \dots, \mathbf{M}_t) (\mathbf{P}(t) \otimes \mathbf{I}). \quad (41)$$

Furthermore, let \mathbf{e}_{t+1} be the $(t+1)$ -dimensional canonical unit vector with $(\mathbf{e}_{t+1})_i = 1$ if $i = t+1$ and $(\mathbf{e}_{t+1})_i = 0$, otherwise. Defining $\mathbf{s}_t = [\mathbf{x}_0^\top, \mathbf{x}_1^\top, \dots, \mathbf{x}_t^\top]^\top$ as the vector of dimension $N(t+1)$ which encompasses all input graph signals, we can write

$$\Phi(t, t-\tau+1) \mathbf{x}_{t-\tau} = (\mathbf{e}_{t+1}^\top \otimes \mathbf{I}) \mathbf{M}_N(t)^\tau \mathbf{s}_t. \quad (42)$$

Since $\mathbf{M}_N(t)$ is not symmetric, instead of the eigenvalue decomposition, we derive the ARMA₁ response using the singular value decomposition. Let $\sigma_i(t)$, $\mathbf{u}_i(t)$, and $\mathbf{v}_i(t)$, be the i th singular value, left and right singular vectors of $\mathbf{M}_N(t)$, where the index i goes from 1 to $N(t+1)$. Substituting (42) into each of the terms of (40) and rearranging the sums, we get

$$\begin{aligned} \varphi \sum_{\tau=0}^t \psi^\tau \Phi(t, t-\tau+1) \mathbf{x}_{t-\tau} &= \varphi (\mathbf{e}_{t+1}^\top \otimes \mathbf{I}) \sum_{\tau=0}^t (\psi \mathbf{M}_N(t))^\tau \mathbf{s}_t, \\ &= (\mathbf{e}_{t+1}^\top \otimes \mathbf{I}) \sum_{i=1}^{N(t+1)} \varphi \frac{1 - (\psi \sigma_i(t))^{t+1}}{1 - \psi \sigma_i(t)} \langle \mathbf{s}_t, \mathbf{v}_i(t) \rangle \mathbf{u}_i(t), \end{aligned} \quad (43)$$

similarly,

$$\begin{aligned} \psi^{t+1} \boldsymbol{\Phi}(t, 0) \mathbf{y}_0 &= (\mathbf{e}_{t+1}^\top \otimes \mathbf{I}) (\psi \mathbf{M}_N(t))^{t+1} (\mathbf{e}_{t+1} \otimes \mathbf{y}_0) \\ &= (\mathbf{e}_{t+1}^\top \otimes \mathbf{I}) \sum_{i=1}^{N(t+1)} (\psi \sigma_i(t))^{t+1} \langle \mathbf{e}_{t+1} \otimes \mathbf{y}_0, \mathbf{v}_i(t) \rangle \mathbf{u}_i(t), \end{aligned} \quad (44)$$

as well as $c \mathbf{x}_t = (\mathbf{e}_{t+1}^\top \otimes \mathbf{I}) \sum_{i=1}^{N(t+1)} c \langle \mathbf{s}_t, \mathbf{v}_i(t) \rangle \mathbf{u}_i(t)$. We can now derive the graph frequency response of the filter by taking the limit over t . For compactness of notation, we drop the time index for all variables in the limit, denoting $\mathbf{s} = \lim_{t \rightarrow \infty} \mathbf{s}_t$, $\mathbf{M}_N = \lim_{t \rightarrow \infty} \mathbf{M}_N(t)$, $\sigma = \lim_{t \rightarrow \infty} \sigma(t+1)$, and so on. From equations (42) - (44) it follows that

$$\mathbf{z} = \lim_{t \rightarrow \infty} \mathbf{z}_t = (\mathbf{e}^\top \otimes \mathbf{I}) \sum_{i=1}^{\infty} \left(\frac{\varphi}{1 - \psi \sigma_i} + c \right) \langle \mathbf{s}, \mathbf{v}_i \rangle \mathbf{u}_i. \quad (45)$$

Notice that the ARMA₁ retains the same graph frequency response as in the time-invariant case (see equation (8)), now expressed in the joint basis of \mathbf{M}_N .

It is not difficult to show that the ARMA₁ graph filter converges asymptotically. Let us denote the error between the filter output at two different time instants $t_1 \geq t_2$ as

$$\epsilon_{t_1, t_2} = \frac{\|\mathbf{z}_{t_1} - \mathbf{z}_{t_2}\|}{x_{\max}}. \quad (46)$$

where $x_{\max} = \max_{t=1, \dots, t_1} \|\mathbf{x}_t\|$ constitutes an upper bound on the energy of the input. We can now claim

Theorem 6. Given the ARMA₁ recursion (40), the error ϵ_{t_1, t_2} between the filter output at time instants t_1 and t_2 is upper-bounded as

$$\begin{aligned} \epsilon_{t_1, t_2} &\leq \|\mathbf{y}_0\| \frac{|\psi \varrho|^{t_1} + |\psi \varrho|^{t_2}}{x_{\max}} + |\varphi| \frac{|\psi \varrho|^{t_2} - |\psi \varrho|^{t_1}}{1 - |\psi \varrho|} \\ &\quad + |c| \frac{\|\mathbf{x}_{t_1-1} - \mathbf{x}_{t_2-1}\|}{x_{\max}}. \end{aligned} \quad (47)$$

Above, ϱ is a constant chosen such that, for every t , $\|\mathbf{M}_t\| \leq \varrho$.

(The proof is deferred to the appendix.)

For simplicity, set $c = 0$. Directly from (47), we then find that for any small positive constant ε , it holds that

$$t_2 \geq \log(\alpha/\varepsilon) \quad \Rightarrow \quad \epsilon_{t_1, t_2} \leq \varepsilon, \quad (48)$$

with $\alpha = 2\|\mathbf{y}_0\|/x_{\max} + |\varphi|/(1 - |\psi \varrho|)$. The theorem therefore asserts that, as long as the stability condition $|\psi \varrho| < 1$ is met, the error decreases exponentially.

The results of Theorem 6 can be extended to the general ARMA_K graph filter. For the parallel implementation, we can proceed in the same way as for the ARMA₁ by considering that the output signal is the sum of K ARMA₁ graph filters. Meanwhile, for the periodic implementation we can see that its form (16), after one cyclic period, is analogous to (39).

VI. NUMERICAL RESULTS

To illustrate our results we simulate two different case-studies: one with a fixed graph and a time-varying graph signal, and one where both the graph and graph signal are time-varying. In the latter case, the ARMA performance is also compared to the state-of-the-art FIR filters designed in a universal manner [6]. With the first case-study, we aim to show how the proposed filters operate on graph signals that have spectral content in both graph and temporal frequency domains. Meanwhile, with the second the goal is to illustrate the ARMA performance when the underlying graph topology is not static anymore, but varies with time.

A. Variations on the Graph Signal

In this subsection, we present simulation results for time-varying signals. We consider a 0.5-bandlimited graph signal \mathbf{u}_t oscillating with a fixed temporal frequency $\pi/10$, meaning that

$$\langle \mathbf{u}_t, \boldsymbol{\phi}_n \rangle = \begin{cases} e^{i\pi t/10} & \text{if } \lambda_n < 0.5 \\ 0 & \text{otherwise,} \end{cases} \quad (49)$$

where λ_n is the n -th eigenvalue of the normalized graph Laplacian and t is the time index. The signal is then corrupted with a second interfering signal \mathbf{v}_t , oscillating with a temporal frequency $9\pi/10$. In addition, the signal is corrupted with i.i.d. Gaussian noise \mathbf{n}_t , with zero mean and variance $\sigma^2 = 0.1$. We then attempt to recover \mathbf{u}_t by filtering it with an ARMA₅ graph filter, effectively canceling the interference \mathbf{v}_t and attenuating the out of band noise. The graph filter is designed to approximate the GFT of \mathbf{u}_t , i.e., to approximate an ideal low-pass filter in the graph domain with cut-off frequency $\lambda_c = 0.5$. Our simulations were conducted using a random geometric graph G composed of 100 nodes placed randomly in a square area, with any two nodes being connected if they are closer than 15% of the maximum distance in the area.

Depending on whether the interference is mutual or not, we distinguish between two scenarios:

i) Mutual signal interference. In this scenario, the interference is self-induced, meaning that \mathbf{v}_t corresponds to the same signal as \mathbf{u}_t , but oscillating at a higher temporal frequency (due for instance to electronics problems). To provide intuition, in Fig. 4.a we show the graph spectral content of \mathbf{u}_0 and $\mathbf{u}_0 + \mathbf{v}_0 + \mathbf{n}_0$. We can see that once corrupted by noise and interference, the graph signal presents significant spectral content across the graph spectrum, thus loosing its bandlimited nature. Meanwhile, Fig. 4.b depicts the real part of the graph spectral content of the filter output after 100 iterations (i.e., well after the initial state \mathbf{y}_0 is forgotten). Even though the figure cannot capture the effect of dynamics (as it solely focuses on $t = 100$), it does show that all frequencies above $\lambda_c = 0.5$ have been attenuated and the interference contribution in band is reduced.

To illustrate the filtering on the temporal frequencies of the signal, in Fig. 5 we show the spectrum of the input and output signal for two representative nodes 1 and 10. To increase visibility, the values in the figure are normalized with respect

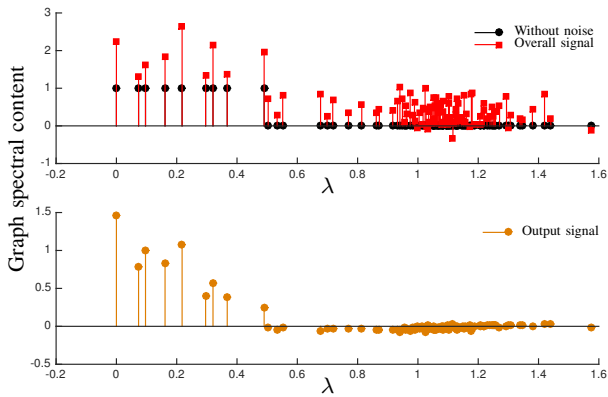


Fig. 4. Graph spectral content of the input signal as well as of the overall signal affected by interference and noise a) (top), and of the filter output signal b) (bottom).

to the maximum. We can see that, for both nodes, the content relative to the interfering frequency $9\pi/10$ of the output signal is attenuated around 20 dB with respect to the main temporal frequency content of $\pi/10$.

ii) *Multiple signal interference.* Let us now consider a more involved scenario, in which the interfering graph signal satisfies

$$\langle \mathbf{v}_t, \phi_n \rangle = e^{i9\pi t/10} e^{-\lambda_n}, \quad (50)$$

i.e., it is a signal having a heat kernel-like graph spectrum oscillating in time with a pulsation $\omega = 9\pi/10$. We will examine two types of errors: i) The first compares for each time t the ARMA₅ output GFT \hat{z}_t to that of the signal of interest

$$e_t^{(total)} = \frac{\|\hat{z}_t - \hat{\mathbf{u}}_t\|}{\|\hat{\mathbf{u}}_t\|}. \quad (51)$$

Achieving a small error $e_t^{(total)}$ is a very challenging problem since an algorithm has to simultaneously overcome the addition of noise and the interference, while at the same time operating in a time-varying setting (see Fig. 6). ii) The second error focuses on interference and compares \mathbf{z}_t to the output \mathbf{z}_t^* of the same ARMA₅ operating on $\mathbf{u}_t + \mathbf{n}_t$ (but not $\mathbf{u}_t + \mathbf{v}_t + \mathbf{n}_t$)

$$e_t^{(interf)} = \frac{\|\hat{z}_t - \hat{z}_t^*\|}{\|\hat{z}_t^*\|}, \quad (52)$$

where \hat{z}_t^* is the GFT of \mathbf{z}_t^* .

We can see that after a few iterations this error becomes relatively small, which means that the output spectrum of the ARMA recursion when the signal is affected by interference is similar to when the interference-less signal is used. This gives a first insight, that using the ARMA recursion we can manage multiple signals on a graph by simply making them orthogonal in the temporal frequency domain. By a specific design of the filter coefficients, one can distributively operate on the graph signal of interest and ignore the others. Such a result cannot be achieved with FIR filters for two reasons: (i) they suffer from handling time-varying input signals, and (ii) the FIR filters do not operate on the temporal frequency content of the graph signals, thus such a distinction between overlapping signals is difficult to achieve.

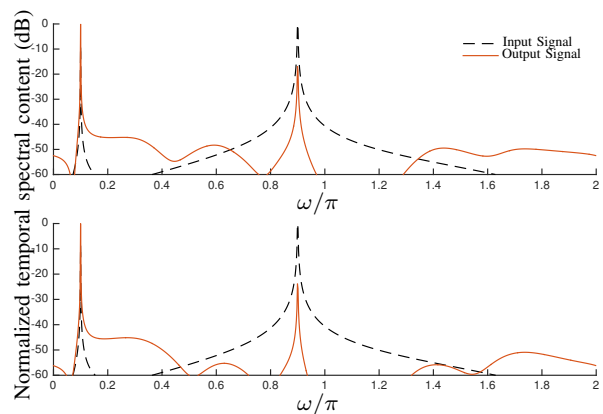


Fig. 5. Time spectral content of the input and output signal for node 1 (top) and node 10 (bottom). The values are normalized with respect to the maximum.

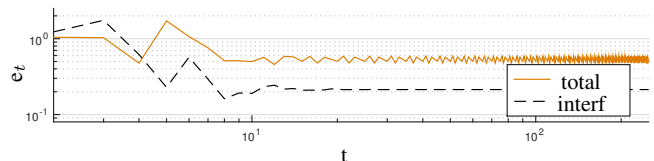


Fig. 6. Error of the ARMA recursion when the time-varying input signal is affected by interference.

The above results illustrate the conclusions of Section V, and also quantify how much we can attenuate the signal at a specific graph/temporal frequency.

B. Variations on the Graph Topology

We examine the influence of graph variations for two filtering objectives. The first, which corresponds to denoising, can be computed *exactly* using ARMA. In the second objective, the graph filter is designed to *approximate* an ideal low-pass graph filter, i.e., a filter that eliminates all graph frequency components higher than some specific λ_c . In addition, we employ two different types of graph dynamics: *random edge failures*, where the edges of a graph disappear at each iteration with a fixed probability, as well as the standard model of *random waypoint* mobility [27]. The above allow us to test and compare universal ARMA and FIR graph filters over a range of scenarios, each having different characteristics.

Exact design (denoising). We simulate the denoising problem (as defined by (20), with $w = 0.5$ and $K = 1$) over the same graph topology of Section VI-A, where the probability that an edge goes down at each time instant is $p = 0.05$. The input signal $\mathbf{x} = \mathbf{u} + \mathbf{n}$ is given by a linear combination of a smooth signal \mathbf{u} and noise \mathbf{n} . To ensure that the graph signal is smooth, we set its spectrum as $\langle \mathbf{u}, \phi_n \rangle = e^{-5\lambda_n}$. The noise \mathbf{n} on the other hand is i.i.d. Gaussian distributed with zero mean and unit variance.

To compare the results we calculate the normalized error between the graph filter output and the analytical solution of the optimization problem (20). In Fig. 7, we plot the normalized error of solving the denoising problem via distributed graph filtering. We consider an ARMA₁ graph filter (designed

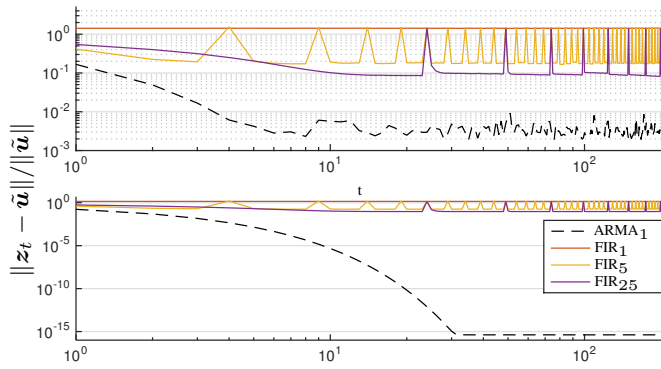


Fig. 7. Normalized error related to the solution of the denoising problem in a distributed way with graph filters. Results relative to random time-varying graph (top) and static graph (bottom). We compare the results of ARMA₁ with different FIR graph filters.

according to Section IV-B) and we compare its performance with the FIR graph filter for different orders. We can see that, for both the random time-varying and static graph the ARMA graph filter gives a lower error with respect to the solution of the optimization problem. As we have seen before, for static graphs the ARMA filter matches correctly the analytical solution. Meanwhile, when the graph is generated randomly it approximates quite well the latter. On the other hand, the performance of the FIR filters is limited by the fact that they only approximate the solution of the optimization problem.

Approximate design (ideal low pass). We use graph filters of increasing orders, specifically $K = 2, 4$ and 6 , to approximate a low-pass graph filter with frequency response $g^*(\lambda) = 1$ if $\lambda < 0.5$, and zero otherwise. We consider a graph with 100 nodes living in a box of 1000×1000 meters, with a communication range of 180 meters. We assume that the nodes will move in the area by a random waypoint model [27] with a constant speed selected in $[0, 3]$ m/s.

We start with a scenario where only the graph topology changes in time whereas the graph signal remains invariant. Then, we simulate a more general case, where both the graph topology and the graph signal are time-varying. For both scenarios, we perform 20 distinct runs, each lasting 10 minutes and consisting of 600 iterations (one iteration per second). We then compare the response error $\|g - g^*\| / \|g^*\|$ at convergence (after 100 iterations), of the ARMA filters with that of the analogous FIR filters.

Time-varying graph, constant graph signal. For this scenario, x is a random vector with entries selected uniformly distributed in $[0, 1]$. In Fig. 8 (top) we show the response error for increasingly higher node speeds. As expected, the error increases with speed. Nevertheless, the ARMA filters show a better performance in comparison to their analogous FIR filters. This indicates that the proposed approach handles better time-varying settings than the FIR filters. Further, we can see that higher order ARMA filters approximate better the desired frequency response (smaller error) when the graph is static. On the other hand, when mobility is present, higher order ARMA recursions lead to a rough approximation due to

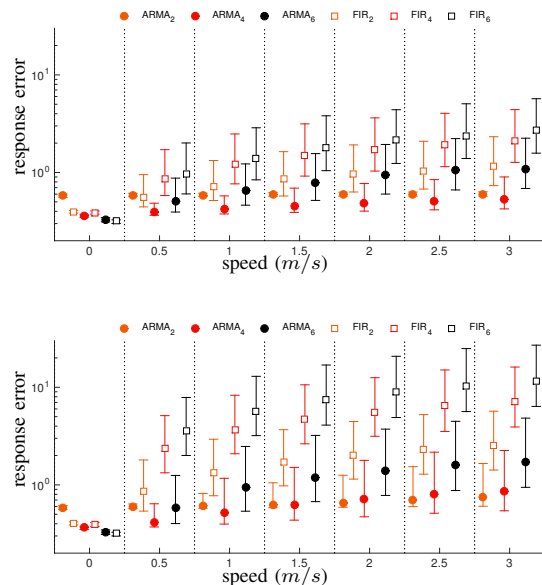


Fig. 8. The effects of the variations only on the graph topology (top) and on both graph and graph signal (bottom). The response error is calculated as $\|g(\lambda) - g^*(\lambda)\| / \|g^*(\lambda)\|$. Each error bar shows the standard deviation of the approximation error over 10 runs. A small horizontal offset is included to improve visibility.

their slower convergence and the fact that the poles go closer to the unit circle (larger coefficients).

Time-varying graph and graph signal. To conclude, we simulate the more general case where both the graph structure and the graph signal change in time. Simulating a target tracking scenario, we let the signal at each node take a value of zero, unless a node was within 100 meters from a target point, residing at the middle of the 1000×1000 meter simulation area, in which case the node's value was set to one. In Fig. 8 (bottom) we show the response error as a function of the node's speed. It is not surprising that letting the graph signal change over time makes the graph filtering problem harder and the corresponding errors of all graph filters larger. Nevertheless, also in this case we can see that the proposed ARMA approach tolerates better time-variations compared to FIR filters.

VII. CONCLUSIONS

In this work, we present the ARMA recursion as a potential algorithm to implement IIR graph filters in a distributed way. We show two different options to approximate any desired graph frequency mask with an ARMA filter of order K , namely a parallel and periodic implementation. Our Shank-based design method shows experimentally that the obtained filters are stable and they can approximate arbitrary well any desired graph frequency response. Furthermore, they are characterized by a linear convergence. Moreover, ARMA filters give an exact solution for two main graph filtering tasks, (i) graph denoising and (ii) graph signal interpolation. Characterized by a rational frequency response, ARMA graph filters can track time-varying input signals. In this case, we show that our filter naturally extends to a 2-dimensional filter operating in the graph-frequency and in the time-frequency domain as well. In this way, we can filter the signal in a

distributed way jointly in both domains instead of operating on each of them separately which leads to higher costs. We also show that this approach is limited by the fact that there is a connection between the poles in the graph domain and those in the Z-domain. Further, we characterize the ARMA recursion when also the graph structure varies in time and we show that the linear convergence is guaranteed also in this environment. Simulation results, quantify the analytical solution and show that the proposed approach outperforms the state of the art FIR graph filters, in both static and time-varying scenarios.

Our future research will be based on finding analytical stable design methods for both 1 and 2-dimensional ARMA recursions. Furthermore, we are also interested to extend the proposed 2-dimensional graph filter to a separable case in order to obtain a disjoint filter design in each domain.

APPENDIX

Proof of Theorem 4

The recursion of a parallel ARMA_K with time-varying input is

$$\mathbf{y}_{t+1}^{(k)} = \psi^{(k)} \mathbf{M} \mathbf{y}_t^{(k)} + \varphi^{(k)} \mathbf{x}_t \quad (\forall k) \quad (53a)$$

$$\mathbf{z}_{t+1} = \sum_{k=1}^K \mathbf{y}_{t+1}^{(k)} + c \mathbf{x}_t, \quad (53b)$$

where $\mathbf{y}_t^{(k)}$ is the state of the k th ARMA₁, whereas \mathbf{x}_t and \mathbf{z}_t are the input and output graph signals, respectively. Using the Kronecker product the above takes the more compact form

$$\mathbf{y}_{t+1} = (\Psi \otimes \mathbf{M}) \mathbf{y}_t + \varphi \otimes \mathbf{x}_t \quad (54a)$$

$$\mathbf{z}_{t+1} = (\mathbf{1}^\top \otimes \mathbf{I}_N) \mathbf{y}_{t+1} + c \mathbf{x}_t, \quad (54b)$$

with $\mathbf{y}_t = (\mathbf{y}_t^{(1)}, \mathbf{y}_t^{(2)}, \dots, \mathbf{y}_t^{(K)})^\top$ the $NK \times 1$ stacked state vector, $\Psi = \text{diag}(\psi^{(1)}, \psi^{(2)}, \dots, \psi^{(K)})$ a diagonal $K \times K$ coefficient matrix, $\varphi = (\varphi^{(1)}, \varphi^{(2)}, \dots, \varphi^{(K)})^\top$ a $K \times 1$ coefficient vector, and $\mathbf{1}$ the $K \times 1$ one-vector. We therefore have

$$\begin{aligned} \mathbf{y}_{t+1} &= (\Psi \otimes \mathbf{M})^t \mathbf{y}_0 + \sum_{\tau=0}^t (\Psi \otimes \mathbf{M})^\tau (\varphi \otimes \mathbf{x}_{t-\tau}) \\ &= (\Psi^t \otimes \mathbf{M}^t) \mathbf{y}_0 + \sum_{\tau=0}^t (\Psi^\tau \varphi) \otimes (\mathbf{M}^\tau \mathbf{x}_{t-\tau}). \end{aligned}$$

Notice that, when the stability condition $\|\psi^{(k)} \mathbf{M}\| < 1$ is met, $\lim_{t \rightarrow \infty} \|(\Psi^t \otimes \mathbf{M}^t) \mathbf{y}_0\| = 0$. Hence, for sufficiently large t , the ARMA_k output is

$$\begin{aligned} \lim_{t \rightarrow \infty} \mathbf{z}_{t+1} &= \lim_{t \rightarrow \infty} \sum_{\tau=0}^t (\mathbf{1}^\top \otimes \mathbf{I}_N) (\Psi^\tau \varphi) \otimes (\mathbf{M}^\tau \mathbf{x}_{t-\tau}) + c \mathbf{x}_t \\ &= \lim_{t \rightarrow \infty} \sum_{\tau=0}^t (\mathbf{1}^\top \Psi^\tau \varphi) \otimes (\mathbf{M}^\tau \mathbf{x}_{t-\tau}) + c \mathbf{x}_t \\ &= \lim_{t \rightarrow \infty} \sum_{\tau=0}^t \sum_{k=1}^K \varphi^{(k)} \left(\psi^{(k)} \mathbf{M} \right)^\tau \mathbf{x}_{t-\tau} + c \mathbf{x}_t, \end{aligned}$$

where we have used the Kronecker product property $(\mathbf{A} \otimes \mathbf{B})(\mathbf{C} \otimes \mathbf{D}) = (\mathbf{AC}) \otimes (\mathbf{BD})$ and expressed the Kronecker product as the sum of K terms. The transfer matrix $\mathbf{H}(z)$

is obtained by taking the Z-transform in both sides and re-arranging the terms

$$\mathbf{H}(z) = z^{-1} \sum_{k=1}^K \varphi^{(k)} \sum_{\tau=0}^{\infty} \left(\psi^{(k)} \mathbf{M} \right)^\tau z^{-\tau} + cz^{-1}.$$

Finally, applying the GFT and using the properties of geometric series we obtain the joint transfer function in closed-form expression

$$\begin{aligned} H(z, \mu) &= z^{-1} \sum_{k=1}^K \varphi^{(k)} \sum_{\tau=0}^{\infty} \left(\psi^{(k)} \mu \right)^\tau z^{-\tau} + cz^{-1} \\ &= \sum_{k=1}^K \frac{\varphi^{(k)} z^{-1}}{1 - \psi^{(k)} \mu z^{-1}} + cz^{-1} \end{aligned}$$

and our claim follows.

Proof of Theorem 5

Expanding recursion (14) for a time varying input signal, we find that at the end of the i -th period, the filter output is $\mathbf{z}_{iK} = \mathbf{y}_{iK} + c \mathbf{x}_{iK-1}$, where

$$\mathbf{y}_{iK} = \prod_{k=iK-1}^0 \mathbf{M}_k \mathbf{y}_0 + \sum_{k=0}^{iK-1} \left(\prod_{\tau=iK-1}^{t+1} \mathbf{M}_\tau \right) \varphi_k \mathbf{x}_k.$$

For sufficiently large i and assuming that the stability condition of Theorem 3 holds, the first term approaches the zero vector and can be ignored without any loss of generality.

We proceed by restricting the input graph signal to $\mathbf{x}_{iK} = x_{iK} \phi$, where μ, ϕ is an eigenpair of \mathbf{M} (similarly $\mathbf{y}_{iK} = y_{iK} \phi$ and $\mathbf{z}_{iK} = z_{iK} \phi$). For compactness we introduce the shorthand notation $\mu_k = \theta_k + \mu \psi_k$ and $M = \prod_{\tau=0}^{K-1} \mu_\tau$. We then have

$$y_{iK} = \sum_{k=0}^{iK-1} \left(\prod_{\tau=k+1}^{iK-1} \mu_\tau \right) \varphi_k x_k,$$

which, after taking the Z-transform, becomes

$$\begin{aligned} \frac{Y(z)}{X(z)} &= \sum_{k=0}^{iK-1} \left(\prod_{\tau=k+1}^{iK-1} \mu_\tau \right) \varphi_k z^{k-iK} \\ &= \sum_{j=0}^{i-1} M^{i-j-1} z^{(j-i)K} \left(\sum_{k=0}^{K-1} \left(\prod_{\tau=k+1}^{K-1} \mu_\tau \right) \varphi_k z^k \right). \end{aligned}$$

The last step exploited the periodicity of coefficients in order to group the common terms of periods $j = 1, \dots, i-1$. In the limit, the first term approaches

$$\begin{aligned} \lim_{i \rightarrow \infty} \sum_{j=0}^{i-1} M^{i-j-1} z^{(j-i)K} &= \lim_{i \rightarrow \infty} M^{-1} \sum_{j=0}^{i-1} \left(\frac{M}{z^K} \right)^{i-j} \\ &= \frac{1}{z^K - M}. \end{aligned}$$

Putting everything together, we find that the joint transfer function of the filter is

$$H(z, \mu) = \frac{Z(z)}{X(z)} = \frac{\sum_{k=0}^{K-1} \left(\prod_{\tau=k+1}^{K-1} \mu_\tau \right) \varphi_k z^k}{z^K - M} + cz^{-1}$$

and, after normalization, the claim follows.

Proof of Theorem 6

We start the proof by substituting the expression (40) for t_1 and t_2 into the numerator of (46). Then, we can write

$$\begin{aligned} \|\mathbf{z}_{t_1+1} - \mathbf{z}_{t_2+1}\| &= \|\psi^{t_1+1}\Phi(t_1, 0)\mathbf{y}_0 - \psi^{t_2+1}\Phi(t_2, 0)\mathbf{y}_0 \\ &+ \varphi \sum_{\tau=0}^{t_1} \psi^\tau \Phi(t_1, t_1 - \tau + 1)\mathbf{x}_{t_1-\tau} + c\mathbf{x}_{t_1} \\ &- \varphi \sum_{\tau=0}^{t_2} \psi^\tau \Phi(t_2, t_2 - \tau + 1)\mathbf{x}_{t_2-\tau} - c\mathbf{x}_{t_2}\|. \end{aligned} \quad (55)$$

Rearranging the terms, we have

$$\begin{aligned} \|\mathbf{z}_{t_1+1} - \mathbf{z}_{t_2+1}\| &= \|\psi^{t_1+1}\Phi(t_1, 0)\mathbf{y}_0 - \psi^{t_2+1}\Phi(t_2, 0)\mathbf{y}_0 \\ &+ \varphi \sum_{\tau=t_2+1}^{t_1} \psi^\tau \Phi(t_1, t_1 - \tau + 1)\mathbf{x}_{t_1-\tau} \\ &+ c(\mathbf{x}_{t_1} - \mathbf{x}_{t_2})\|. \end{aligned} \quad (56)$$

By using the Cauchy-Schwarz property, the triangle inequality of the spectral norm, and a uniform bound ϱ on the eigenvalues of matrices \mathbf{M}_t , the above expression simplifies

$$\begin{aligned} \|\mathbf{z}_{t_1+1} - \mathbf{z}_{t_2+1}\| &\leq \left(|\psi\varrho|^{t_1+1} + |\psi\varrho|^{t_2+1} \right) \|\mathbf{y}_0\| \\ &+ |\varphi| \sum_{\tau=t_2+1}^{t_1} |\psi\varrho|^\tau \|\mathbf{x}_{t_1-\tau}\| + |c| \|\mathbf{x}_{t_1} - \mathbf{x}_{t_2}\|. \end{aligned} \quad (57)$$

Leveraging the fact that $|\psi\varrho| < 1$, as well as that $\|\mathbf{x}_t\| \leq x_{max}$ for every t , we can express the sum in a closed form

$$\sum_{\tau=t_2+1}^{t_1} |\psi\varrho|^\tau \|\mathbf{x}_{t_1-\tau}\| \leq x_{max} \left(\frac{|\psi\varrho|^{t_2+1} - |\psi\varrho|^{t_1+1}}{1 - |\psi\varrho|} \right). \quad (58)$$

We obtain the desired bound on ϵ_{t_1, t_2} by dividing the above expressions with x_{max} and adjusting the indexes.

REFERENCES

- [1] A. Loukas, A. Simonetto, and G. Leus, "Distributed Autoregressive Moving Average Graph Filters," *Signal Processing Letters*, vol. 22, no. 11, pp. 1931–1935, 2015.
- [2] D. I. Shuman, S. K. Narang, P. Frossard, A. Ortega, and P. Vandergheynst, "The Emerging Field of Signal Processing on Graphs: Extending High-Dimensional Data Analysis to Networks and Other Irregular Domains," *IEEE Signal Processing Magazine*, vol. 30, no. 3, pp. 83–98, 2013.
- [3] A. Sandryhaila and J. M. F. Moura, "Discrete Signal Processing on Graphs," *Transactions on Signal Processing*, vol. 61, no. 7, pp. 1644–1656, 2013.
- [4] M. G. Rabbat and V. Gripon, "Towards a Spectral Characterization of Signal Supported on Small-World Networks," in *Proceedings of the 2014 IEEE International Conference on Acoustic, Speech and Signal Processing (ICASSP)*, Firenze, Italy, May 2014, pp. 4826 – 4830.
- [5] F. Zhang and E. R. Hancock, "Graph spectral image smoothing using the heat kernel," *Pattern Recognition*, vol. 41, no. 11, pp. 3328–3342, 2008.
- [6] D. I. Shuman, P. Vandergheynst, and P. Frossard, "Chebyshev polynomial approximation for distributed signal processing," in *International Conference on Distributed Computing in Sensor Systems and Workshops (DCOSS)*. IEEE, 2011, pp. 1–8.
- [7] A. J. Smola and R. Kondor, "Kernels and regularization on graphs," in *Learning theory and kernel machines*. Springer, 2003, pp. 144–158.
- [8] X. Zhu, Z. Ghahramani, and J. Lafferty, "Semi-supervised learning using gaussian fields and harmonic functions," in *Proceedings of the 20th International Conference on Machine Learning (ICML-2003) Volume 2*, vol. 2. AIAA Press, 2003, pp. 912–919.
- [9] M. Belkin and P. Niyogi, "Semi-supervised learning on riemannian manifolds," *Machine learning*, vol. 56, no. 1-3, pp. 209–239, 2004.
- [10] S. K. Narang, A. Gadde, and A. Ortega, "Signal processing techniques for interpolation in graph structured data," in *Acoustics, Speech and Signal Processing (ICASSP), 2013 IEEE International Conference on*. IEEE, 2013, pp. 5445–5449.
- [11] A. Loukas, M. A. Zúñiga, I. Protonotarios, and J. Gao, "How to identify global trends from local decisions? Event Region Detection on Mobile Networks," in *International Conference on Computer Communications (INFOCOM)*, 2014.
- [12] D. K. Hammond, P. Vandergheynst, and R. Gribonval, "Wavelets on graphs via spectral graph theory," *Applied and Computational Harmonic Analysis*, vol. 30, no. 2, pp. 129–150, 2011.
- [13] X. Dong, D. Thanou, P. Frossard, and P. Vandergheynst, "Learning graphs from signal observations under smoothness prior," *arXiv preprint arXiv:1406.7842*, 2014.
- [14] A. Sandryhaila, S. Kar, and J. M. F. Moura, "Finite-time distributed consensus through graph filters," in *International Conference on Acoustics, Speech and Signal Processing (ICASSP)*. IEEE, 2014, pp. 1080–1084.
- [15] S. Safavi and U. A. Khan, "Revisiting Finite-Time Distributed Algorithms via Successive Nulling of Eigenvalues," *Signal Processing Letters, IEEE*, vol. 22, no. 1, pp. 54–57, 2015.
- [16] S. Segarra, A. G. Marques, and A. Ribeiro, "Distributed implementation of linear network operators using graph filters," in *53rd Allerton Conf. on Commun. Control and Computing*, Sept. 2015.
- [17] A. Loukas, M. Cattani, M. A. Zúñiga, and J. Gao, "Graph Scale-Space Theory for Distributed Peak and Pit Identification," in *International Conference on Information Processing in Sensor Networks (IPSN)*. ACM/IEEE, 2015.
- [18] X. Shi, H. Feng, M. Zhai, T. Yang, and B. Hu, "Infinite Impulse Response Graph Filters in Wireless Sensor Networks," *Signal Processing Letters, IEEE*, 2015.
- [19] A. Loukas, M. A. Zúñiga, M. Woehle, M. Cattani, and K. Langendoen, "Think Globally, Act Locally: On the Reshaping of Information Landscapes," in *International Conference on Information Processing in Sensor Networks (IPSN)*. ACM/IEEE, 2013.
- [20] S. Boyd and L. Vandenberghe, *Convex Optimization*. Cambridge University Press, sec. 9.3, pp. 466–475, 2004.
- [21] J. L. Shanks, "Recursion filters for digital processing," *Geophysics*, vol. 32, no. 1, pp. 33–51, 1967.
- [22] S. Chen, A. Sandryhaila, J. M. F. Moura, and J. Kovacevic, "Signal Denoising on Graphs via Graph Filtering," in *Global Conference on Signal and Information Processing (GlobalSIP)*. IEEE, 2015.
- [23] C. Zhang, D. Florencio, and P. Chou, "Graph signal processing - a probabilistic framework," Tech. Rep. MSR-TR-2015-31, April 2015. [Online]. Available: <http://research.microsoft.com/apps/pubs/default.aspx?id=243326>
- [24] Y. Mao, G. Cheung, and Y. Ji, "Image interpolation for dibr viewsynthesis using graph fourier transform," in *3DTV-Conference: The True Vision-Capture, Transmission and Display of 3D Video*, ser. 3DTV-CON. IEEE, 2014, pp. 1–4.
- [25] T. Zhang, A. Popescul, and B. Dom, "Linear prediction models with graph regularization for web-page categorization," in *Proceedings of the 12th ACM SIGKDD international conference on Knowledge discovery and data mining*. ACM, 2006, pp. 821–826.
- [26] B. Touri, "Product of Random Stochastic Matrices and Distributed Averaging," Ph.D. dissertation, University of Illinois at Urbana Champaign, 2011.
- [27] N. Aschenbruck, R. Ernst, E. Gerhards-Padilla, and M. Schwamborn, "Bonnmotion: A mobility scenario generation and analysis tool," in *International ICST Conference on Simulation Tools and Techniques*, ser. SIMUtools. ICST, 2010.